

# Optimization of heat treatment process for cast steel 50SL

*E. A. Pismennyi*, Postgraduate Student of the Dept. “Engineering Technology”<sup>1</sup>, e-mail: pismennyi.eug@mail.ru;

*A. M. Markov*, Dr. Eng., Prof., Rector, Dept. “Engineering Technology”<sup>1</sup>, e-mail: andmarkov@inbox.ru;

*A. I. Augstkaln*, Postgraduate Student of the Dept. of Physics, Assistant of the Dept. of Mechanical Engineering Technologies and Equipment<sup>1</sup>, e-mail: Augstkaln-a@yandex.ru;

*V. B. Deev\**, Dr. Eng., Prof., School of Mechanical Engineering and Automation<sup>2</sup>, Chief Researcher<sup>3</sup>, Prof. of the Dept. of Metal Forming<sup>4</sup>, e-mail: deev.vb@mail.ru

<sup>1</sup> Polzunov Altai State Technical University (Barnaul, Russia)

<sup>2</sup> Wuhan Textile University (Wuhan, China)

<sup>3</sup> Vladimir State University named after Alexander and Nikolay Stoletovs (Vladimir, Russia)

<sup>4</sup> National University of Science and Technology MISIS (Moscow, Russia)

\* Corresponding author: deev.vb@mail.ru

The attainment of the necessary mechanical and operational properties in cast steels typically involves heat treatment, leading to a consequent increase in the final part’s cost by 30–60 %. In this study, we have enhanced the heat treatment process for cast steel 50SL, streamlining the entire procedure into a single cycle rather than the conventional two-cycle method required for cast steels. This process involves homogenization annealing followed by subsequent quenching through reheating, alongside appropriate tempering to achieve the desired mechanical and operational characteristics. Through our research, it was demonstrated that the optimal heat treatment regimen for cast components of railway cars involves heating to 950 °C, maintaining this temperature, followed by controlled cooling in a furnace to 850 °C, with a brief hold before final cooling in water. Subsequent tempering is conducted at 350 °C for 2 hours. This refined heat treatment protocol, consolidated into a single thermal heating process, significantly reduces the duration of the entire heat treatment cycle by 2.4 times and slashes costs by a factor of 4. Consequently, products fabricated from steel 50SL exhibit mechanical properties 10–12 % superior to those achieved through the conventional heat treatment approach, comprising annealing with furnace cooling, reheating for quenching, and subsequent tempering.

**Key words:** heat treatment, cast steel 50SL, structural-phase state, friction wedge.

**DOI:** 10.17580/cisisr.2024.02.08

## Introduction

Enhancing the efficiency of freight transportation necessitates the implementation of modern technologies and components. Improving the efficiency and functionality of freight car bogie parts can be accomplished through limited alterations in design parameters and material properties related to friction wedges [1–5]. The friction wedge, situated within the vibration damping unit of the freight car bogies, serves to prevent the car body from swaying during motion. In this context, the effectiveness of the wedges is determined by qualities such as strength and durability. Traditionally, the enhancement of any design is assessed through simplification, increased manufacturability, material substitution, and reduced metal consumption [6–8]. Consequently, particular attention is directed towards enhancing the quality and operational reliability of railway castings [9–11].

Earlier, during the process of creating and designing a new friction wedge for a vibration damping unit in a freight car bogie, a novel wedge design was developed. A utility model patent was obtained, accompanied by the creation of a drawing and technical specifications for further development. By optimizing the design parameters of the friction wedge, the contact area of its vertical working surface was increased by 8 % compared to similar models. This enhancement significantly bolstered the service life and reliability of the developed friction wedge design [12, 13]. To further enhance strength and wear resistance, it is suggested to manufacture the friction wedge using medium-carbon low-alloy steel 50SL, the chemical composition of which is detailed in **Table 1**.

The “friction wedge” part features a complex three-dimensional shape that can only be achieved through casting,

**Table 1. Chemical composition of steel 50SL according to GOST 977-88**

Steel grade	Mass percentage of elements, %								
	C	Si	Mn	Ni	S	P	Cr	Cu	Al
50SL	0.46–0.57	1.2–1.6	0.4–0.7	0.25 max	0.03 max	0.025 max	0.35 max	0.2 max	0.2 max

presenting a significant challenge for alternative manufacturing methods. Additionally, stringent criteria are imposed on both the design and material of the friction wedge. Specifically, the structural integrity of the friction wedge must withstand loads of 2.5 MN without undergoing plastic deformation. The primary material requirement for the friction wedge is exceptional resistance to abrasive-frictional wear, while maintaining a hardness within the range of 260 to 340 HB. Typically, these properties are attained through heat treatment procedures, encompassing homogenization annealing of castings, quenching with reheating, and subsequent tempering at temperatures ranging from 350 to 450 °C [14–16]. However, such heat treatment significantly elevates the cost of the final “friction wedge” part. Moreover, due to the extensive duration of the annealing process, often spanning tens of hours, the production cycle of “friction wedge” components is considerably prolonged, with homogenization annealing of castings alone occupying approximately 30 to 45 % of the overall production time.

Thus, optimizing the heat treatment regime to reduce its duration enables, on the one hand, cost reduction of the product, and on the other hand, enhancement of labor productivity, consequently lowering the cost of finished products for the end consumer. To streamline the technological process and diminish the expense of finished castings for a friction wedge in a railway car bogie crafted from 50SL steel, it would be prudent to amalgamate the annealing and heating for quenching operations into a singular procedure. This consolidation eliminates the lengthiest (and correspondingly costliest) cooling stage, which occurs alongside the furnace during annealing. Prior investigations and scrutiny of regulatory literature concerning analogous 50SL steel grades [17] suggest the feasibility of optimizing the technological parameters of heat treatment, facilitating the integration of annealing and quenching operations within a single heat treatment cycle.

The purpose of this work is to optimize the heat treatment regime in order to obtain a satisfactory complex of strength and ductility of castings from steel 50SL in one thermal cycle, excluding preliminary annealing of the castings.

### Materials and Methods

An analysis of literature and patent sources shows that the combination of the operations of annealing castings and heating for quenching is successfully used mainly in foreign industry. The process that is essentially the closest is presented in [7, 17]. For steel 50SL this solution was revised: two-stage heating to the austenitization temperature was carried out to a temperature of 950 °C ( $A_{c3} + (120–140) °C$ ) with holding at this temperature for 1.5–2 hours (4/5 of the total holding time), then the holding temperature was reduced to 850–870 °C and kept at this temperature for 0.3–0.4 hours. The total time of the two-stage high-temperature holding, including the time to reduce the temperature in the furnace chamber, did not exceed 3–3.5 hours. At the end of the high-temperature exposure, the parts were cooled in water and tempered for 2–2.5 hours at a temperature of 330–370 °C. As a result of this heat treatment, the micro-

structure of friction wedge castings made of steel 50SL is bainite with a small amount (about 3–7 wt. %) of acicular ferrite, the average grain size corresponds to 8–9 points. The hardness of the friction wedge castings after heat treatment was  $340 \pm 40$  HB.

To ascertain the optimal heat treatment process concerning the desired hardness model experiments were conducted. These experiments involved cutting samples measuring  $15 \times 15 \times 70$  mm from the friction wedge casting body, which were subsequently subjected to heat treatment under following conditions:

Mode No. 1 – heating to 850 °C, holding for 2.5 hours, cooling with the furnace to 250 °C, then in air; Mode No. 2 – heating to 950 °C, holding for 2 hours, cooling with the furnace to 850 °C, holding for 0.3 hours, cooling in water; Mode No. 3 – heating to 950 °C, holding for 2 hours, cooling with the furnace to 850 °C, holding for 0.3 hours, cooling in oil; Mode No. 4 – heating to 850 °C, holding for 2.5 hours, cooling in water; Mode No. 5 – heating to 850 °C, holding for 2.5 hours, cooling in oil; Mode No. 6 – heating to 950 °C, holding for 2.5 hours, cooling in still air; Mode No. 7 – heating to 950 °C, holding for 2 hours, cooling with the furnace to 850 °C, holding for 0.3 hours, cooling in water; tempering at 350 °C for 2 hours; Mode No. 8 – heating to 950 °C, holding for 2 hours, cooling with the furnace to 850 °C, holding for 0.3 hours, cooling in oil; tempering at 350 °C for 2 hours.

At least six samples were subjected to heat treatment in each mode. These samples were extracted from workpieces treated under all modes for hardness measurement. Fractographic, diffractometric, and metallographic studies were conducted.

Cutting templates for microstructural studies was carried out on a precision cutting machine “Microcut-201”, then the templates were pressed into a bakelite compound using a metallographic press “MetaPress”. Grinding and polishing were carried out on an automatic grinding and polishing machine “DigiPrep-P”. Metallographic analysis was performed using a Carl Zeiss Axio Observer Z1m metallographic microscope and the ThixoMet PRO software package according to methods [18–20].

The average grain score was measured according to GOST 5639-82. Hardness of samples was studied using hardness tester TR 5006 (by Rockwell, GOST 23677-79) with a test load up to 1471 N (GOST 9013-59). The phase composition of the samples was determined using a DRON-6.0 X-ray diffractometer. Studies of the fine structure of the samples were carried out on a Hitachi SU3800 scanning electron microscope using the EDS QUANTAX micro-X-ray spectral analysis method (Bruker) in the secondary (SE) and back-scattered (BSE) electron modes.

### Results and Discussion

**Table 2** shows the main characteristics of the obtained structure of samples cut from 50SL steel castings, depending on the parameters of the heat treatment modes.

The structure of the sample heat-treated according to mode No. 1 comprises a ferrite-pearlite mixture, characterized by the presence of ferrite in both isolated grains and

Mode	Parameters of heat treatment modes	Main characteristics of the structure
1	Heating to 850 °C, holding for 2.5 hours, cooling in a furnace to 250 °C, then in air	ferrite-pearlite mixture, average grain grade – 6
2	Heating to 950 °C, holding for 2 hours, cooling with the furnace to 850 °C, holding for 0.3 hours, cooling in water	hardened martensite, average grain grade – 9
3	Heating to 950 °C, holding for 2 hours, cooling with the furnace to 850 °C, holding for 0.3 hours, cooling in oil	hardened martensite and troostite, average grain grade – 9
4	Heating to 850 °C, holding for 2.5 hours, cooling in water	hardened martensite, average grain grade 7–8
5	Heating to 850 °C, holding for 2.5 hours, cooling in oil	troostite + martensite (20 vol. %) average grain grade – 8
6	Heating to 950 °C, holding for 2.5 hours, cooling in still air	ferrite-pearlite mixture, ferrite is represented in the form of individual grains; average grain grade – 9
7	Heating to 950 °C, holding for 2 hours, cooling with the furnace to 850 °C, holding for 0.3 hours, cooling in water. Tempering at 350 °C, 2 hours	tempered martensite, average grain grade – 10
8	Heating to 950 °C, holding for 2 hours, cooling with the furnace to 850 °C, holding for 0.3 hours, cooling in oil. Tempering at 350 °C, 2 hours	tempered martensite, average grain grade – 10

as a network along the former austenite grain boundaries. The resulting annealed grain exhibits an average score of 6, while the former austenite grain, upon determination, presents a score of –3.

In contrast, the structure of the sample treated under mode No. 1 manifests hardened martensite, with an average grain score of 9. The scoring of the former austenite grain remains indeterminable. The phase composition of this sample predominantly consists of quenched martensite, although approximately 4–7 vol. % of retained austenite is observed, a presence confirmed through diffraction studies.

The structure of the sample treated under mode No. 3 displays quenched and partially tempered martensite, characterized by an average grain score of 9.

In the case of oil quenching at a temperature of 850 °C, the phase composition of the sample comprises retained austenite, thin-plate pearlite (troostite), and martensite. The structural-phase composition, determined through a combination of metallographic and diffractometric analyses, reveals austenite at approximately 5 vol. %, martensite at about 70 vol. %, and troostite constituting the remainder (approx. 25 vol. %). This indicated phase composition is further corroborated by durometric tests, demonstrating a sample hardness of 57 HRC post-quenching. The presence of retained austenite is notably monitored and confirmed via X-ray diffractometry.

The microstructure of the sample, subjected to treatment under mode No. 4, primarily consists of hardened martensite. However, a distinction lies in the grain size, which in this instance is larger, corresponding to 7–8 points. Although residual austenite in this sample is not observed via optical and electron microscopy in a structurally free state, its presence is distinctly evident in the diffraction patterns of the sample. Hardness measurements reveal the isotropic nature of the structural-phase state post-quenching, with hardness values ranging from 61 to 63 HRC.

In the case of replacing the cooling medium from water to oil (mode No. 5), significant alterations occur in the structural-phase state of samples fabricated from cast steel 50SL. In this scenario, the proportion of martensite does not

exceed 20 vol. %, with the remaining volume of phases, as determined by optical microscopy, corresponding to troostite. Hardness measurements of oil-quenched samples yielded results of 48–52 HRC. Beyond microscopic examination, the structural and phase state of the samples was further validated through diffraction analysis.

The structure of the sample subjected to heat treatment under mode No. 6 manifests as a ferrite-pearlite composite, wherein ferrite exists as discrete grains, with a portion of the ferrite localized as reticular precipitates along the boundaries of the former austenite grain. The resultant grain size averages at 9. The rating of the former austenitic grain corresponds to a value of 7. This structure exhibits lower hardness values at 30–32 HRC compared to hardened samples. Despite literature sources suggesting that a temperature of 950 °C is somewhat elevated based on analogues of steel grades with similar chemical compositions, the chosen temperature, held for 2.5 hours, sufficiently homogenized both the chemical and structural-phase states in one heat treatment cycle, considering the initial structural-phase state inherent to cast steel. Consequently, the need for prolonged homogenization annealing of castings before heat treatment was obviated. The conducted analysis of the phase composition of the sample leads to the assertion that its structural-phase state, on the whole, is in equilibrium, with no significant distortions observed in the crystal lattices of all phases.

The most interesting for the production are the results revealed after application of heat treatment according to modes No. 7 and No. 8, which contribute to obtaining a more uniform structure of the studied samples. Therefore, here it is expedient to analyze in more detail the data obtained by means of phase composition and microstructure studies.

The structure of the sample heat-treated according to mode No. 7 is tempered martensite. In photographs of the microstructure taken at high resolution (**Fig. 1**), a small amount of retained austenite is visible (about 0.7 vol. %). The average grain score, determined by the length of martensite needles, corresponds to 10.

As can be seen from the microstructure shown in Fig. 1, this heat treatment mode made it possible to completely

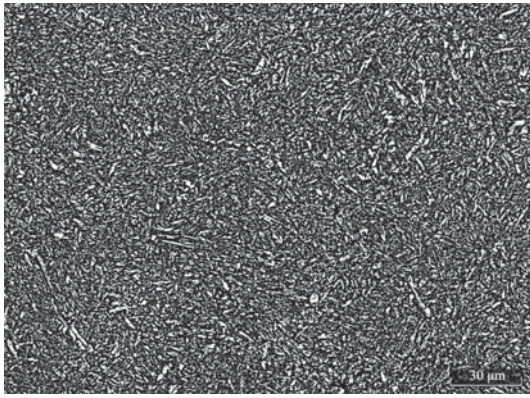


**Fig. 1.** Microstructure of a sample made of steel 50SL, heat-treated according to the mode No. 7

homogenize the chemical composition of the steel in a relatively short time of about 3–3.5 hours and then carry out quenching followed by tempering. Sulfide inclusions are mainly represented by manganese sulfide MnS, oxide inclusions are represented by iron oxide FeO and have predominantly a shape close to globular. The structural state of the sample is tempered martensite; the average length of martensite needles is 18–20  $\mu\text{m}$ .

SEM photographs of the microstructure confirm the data obtained from optical microscopy (Fig. 2). As evident from the presented images, the presence of the martensite phase is affirmed – its needle-like structure is distinctly visible, with an average angle between individual needles of approximately  $63^\circ$ , indicative of the martensite phase. In high-resolution microstructure photographs, cementite deposits can be discerned, exhibiting a shape resembling globules and positioned along the boundaries of martensite needles. The average size of cementite precipitates is approximately 70–90 nm, with individual particles reaching sizes of up to 400 nm; however, their incidence comprises only 0.3 % of the total number of cementite particles. Notably, cementite inclusions with sizes ranging from 70 to 90 nm constitute 92 % of the total number of cementite precipitates.

As evidenced by the diffraction pattern depicted in Fig. 3, the structural-phase state of the sample is in equilibrium, characterized by the presence of ferrite and

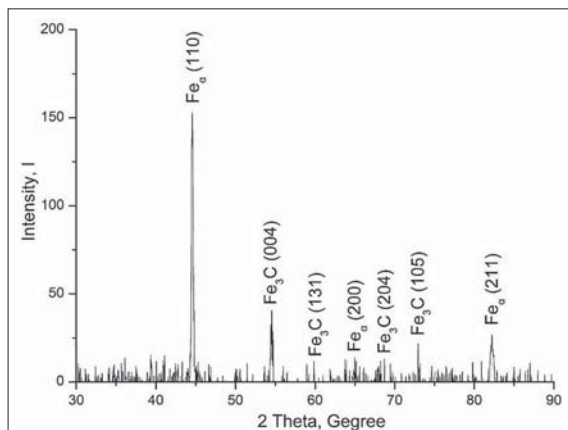


**Fig. 3.** X-ray diffraction pattern of a sample made of steel 50SL, heat-treated according to the mode No. 7

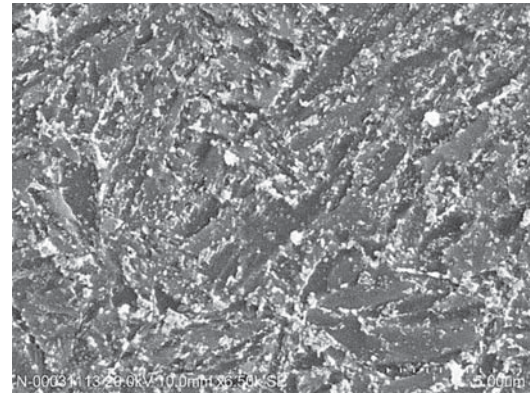


**Fig. 2.** Cementite precipitation along the boundaries of martensitic needles in 50SL steel, heat-treated according to mode No. 7

cementite phases. Notably, there are no reflections indicating retained austenite. The ferrite reflections exhibit slight shifts and broadening, suggesting deformation of its crystal lattice compared to pure ferrite, likely due to the presence of dissolved carbon atoms. Additionally, the characteristic reflections of defect-free cementite indicate the formation of cementite inclusions through diffusion processes during tempering.

The structure of the sample heat-treated according to mode No. 8 is a mixture of ferrite in an amount of 4–6 vol. % and tempered martensite (the rest). In photographs of the microstructure, including those taken at high resolution, retained austenite is not detected. The average grain score, determined by the average length of martensitic needles, is 10. The average ferrite grain score is 11. Based on this, heat treatment mode No. 8 did not allow complete homogenization of the chemical composition of the steel in comparison with mode No. 7, due to the presence of structurally free ferrite. The structural state of the sample is predominantly tempered martensite; the average length of martensite needles is 18–20  $\mu\text{m}$ . In addition to martensite, the samples also contain a ferrite phase, localized in the form of individual island accumulations of ferrite grains up to 15  $\mu\text{m}$  in size.

The microstructure images obtained using SEM also confirm the optical microscopy data (Fig. 4).

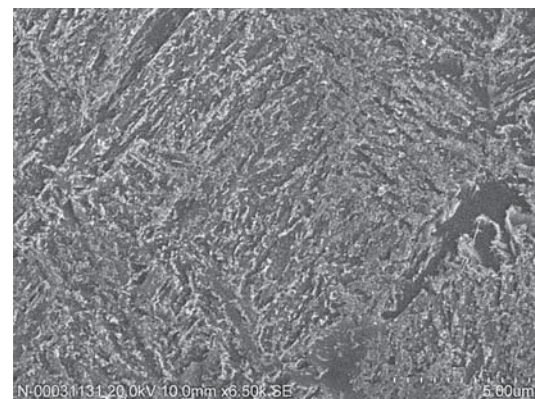


**Fig. 4.** Cementite precipitation along the boundaries of martensitic needles in 50SL steel, heat-treated according to the mode No. 8

In a high-resolution SEM image of the microstructure, cementite precipitates with a globular shape are discernible along the boundaries of martensite needles. The average size of these precipitates ranges from 50 to 60 nm, with individual particles reaching sizes of up to 200 nm. However, the total number of such particles is lower compared to heat treatment mode No. 7. This discrepancy is most likely due to the slower cooling rates experienced by the sample in oil, allowing for greater time for the diffusion redistribution of carbon within the martensite. Consequently, the resulting martensite formed during oil quenching is less defective and less stressed. Subsequent tempering of the oil-hardened sample leads to a less intense redistribution of carbon, resulting in a decrease in the quantity of cementite precipitates along with an increase in their dispersion.

It is worth considering separately the precipitates of the ferrite phase. These precipitates are entirely devoid of cementite precipitates (see Fig. 4), indicating their formation in the higher temperature range prior to the initiation of the martensitic transformation. Consequently, this suggests the diffusion-driven displacement of carbon, concomitant with the formation of the most perfect crystal lattice  $\alpha$ -phases. This assertion finds support in the diffraction data (Fig. 5), where the reflections of the  $\alpha$ -phase and cementite in the diffraction pattern correspond to the states of maximum equilibrium for the studied phases.

Thus, the proposed heat treatment mode No. 7 for cast steel 50SL has significant prospects for increasing production efficiency, reducing costs and improving product quality.

Industrial tests of mode No. 7 of heat treatment of 50SL cast steel have shown that it allows to reduce the time of the complete cycle of heat treatment 2.4 times, and to reduce its cost 4 times. The study of the complex of mechanical properties of products made of 50SL steel showed an increase of 10–12 % in comparison with heat treatment including annealing, cooling with a furnace, quenching with reheating, followed by tempering.


Potential economic benefits from the implementation of the solutions outlined include a reduction in production cycle time while simultaneously providing improved properties

and characteristics of products and, as a result, strengthening the position of enterprises in a competitive market. Of significant interest is the further development of structural applications of 50SL steel after heat treatment according to recommended conditions in the manufacture of various small-sized shaped products of buildings and structures, for example, connectors for assembling various structural elements, etc.

### Conclusions

1. According to the results of the conducted studies of the structural-phase state using optical, scanning electron microscopy and X-ray diffractography, the most optimal structural-phase state is possessed by steel 50SL, heat-treated according to mode No. 7: heating to 950 °C, holding for 2 hours, cooling with the furnace to 850 °C, holding for 0.3 hours, cooling in water. Tempering at 350 °C, 2 hours.

2. Compared with traditional heat treatment, including annealing of castings and then their heat treatment (quenching and subsequent tempering) with reheating, the proposed technology (heat treatment according to mode No. 7) makes it possible to obtain a more uniform microstructure in a shorter time – the full cycle of heat treatment using the proposed technology has a total duration no more than 5 hours, while the full cycle of heat treatment, including annealing of castings with their cooling together with the furnace for 8 hours, quenching with reheating and subsequent tempering, has a duration of at least 12 hours.

3. The developed heat treatment mode for one thermal heating makes it possible to reduce the time of the full heat treatment cycle by 2.4 times, reduce its cost by 4 times and thereby obtain products from steel 50SL, which have a 10–12 % higher set of mechanical properties Compared to the traditionally used heat treatment, consisting of annealing, furnace cooling, quenching with reheating followed by tempering. 

*The research was carried out within the state assignment in the field of scientific activity of the Ministry of Science and Higher Education of the Russian Federation (theme FZUN-2024-0004, state assignment of the VISU).*

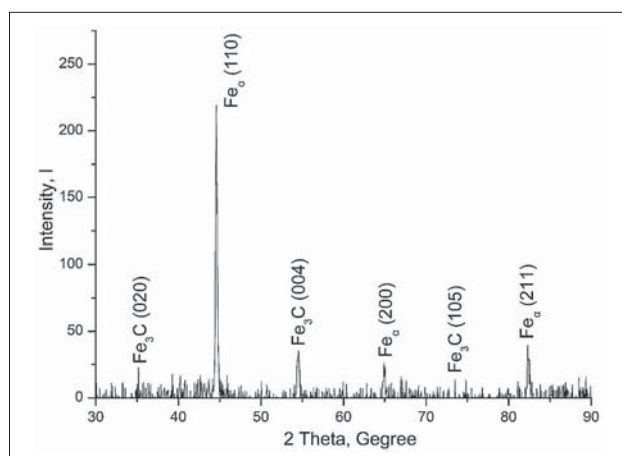


Fig. 5. X-ray diffraction pattern of a sample of 50SL steel, heat-treated according to the mode No. 8

### REFERENCES

- Sun Y. Q., Cole C. Vertical dynamic behavior of three-piece bogie suspensions with two types of friction wedge. *Multibody System Dynamics*. 2008. Vol. 19. pp. 365–382. DOI: 10.1007/s11044-007-9085-z.
- Xu X., Fu M., Xu Z., Chen Z. A new lever-type variable friction damper for freight bogies used in heavy haul railway. *Journal of Modern Transportation*. 2016. Vol. 24. pp. 159–165. DOI: 10.1007/s40534-016-0116-4.
- Yadav O. P., Vyas N. S. The influence of AAR coupler features on estimation of in-train forces. *Railway Engineering Science*. 2023. Vol. 31. pp. 233–251. DOI: 10.1007/s40534-022-00297-8.
- Stichel S. Limit Cycle Behaviour and Chaotic Motions of Two-Axle Freight Wagons with Friction Damping. *Multibody System Dynamics*. 2002. Vol. 8. pp. 243–255. DOI: 10.1023/A:1020990128895.
- Ron'zhin I., Barinova G. P., Grinshpon A. S., Demin Yu. S., Maksimov S. G., Filippov G. A., Kononov A. A. Features of the production of railroad wheels with more durable rims. *Metallurgist*. 2002. Vol. 46. Nos. 11–12. pp. 340–343.

6. Wu Q., Luo S., Cole C. Longitudinal dynamics and energy analysis for heavy haul trains. *Journal of Modern Transportation*. 2014. Vol. 22, pp. 127–136. DOI: 10.1007/s40534-014-0055-x.
7. A913/A913M-11: Standard Specification for High-Strength Low-Alloy Steel Shapes of Structural Quality, Produced by Quenching and Self-Tempering Process (QST). ASTM International, 2011, West Conshohocken.
8. Soldatov V. G., Manuev M. S., Ivashchenkov Y. M., Tupatilov E. A. Optimization of properties of steel 20GL for railway transport castings. *Metal Science and Heat Treatment*. 2007. Vol. 49, p. 417–419. DOI: 10.1007/s11041-007-0079-5.
9. Lebedinskii S. G., Barmina O. V. Analysis of Survivability of Cast Railroad Parts under Operational Loading. *Journal of Machinery Manufacture and Reliability*. 2023. Vol. 52, pp. 486–491. DOI: 10.3103/S1052618823050114.
10. Lebedinskii S. G. Operating Life of Steel in Cast Parts of Rail Transport. *Journal of Machinery Manufacture and Reliability*. 2022. Vol. 51 (Suppl. 1), S36–S41. DOI: 10.3103/S1052618822090096.
11. Bulbuc V., Paleu V., Pricop B., Popa M., Cârlescu V., Cimpoesu N., Bujoreanu L. G. Effects of Dynamic Loading under Extreme Conditions on Wear Resistance of T105Mn120 Castings for Railway Safety Systems. *Journal of Materials Engineering and Performance*. 2021. Vol. 30, pp. 7128–7137. DOI: 10.1007/s11665-021-05837-7.
12. Gabets D. A., Markov A. M., Pismenny E. A., Chertovskikh E. O. Utility model patent No. 194823 of the Russian Federation. Friction wedge of a railway car bogie. No. 1019133574; appl. 10/22/2019; publ. 12/24/2019.
13. Gabets D. A., Gabets A. V., Levkin I. V., Chertovskikh E. O. Certificate of registration of a computer program No. 1020619875. CAD model of the concept of a friction wedge for a freight car bogie. No. 1020618630; appl. 08/06/2020; publ. 08/25/2020.
14. Verdeja González J. I., Fernández-González D., Verdeja González L. F. Physical Metallurgy and Heat Treatment of Steel. Springer Cham. 2023. 332 p. DOI: 10.1007/978-3-031-05702-1.
15. Berns H., Theisen W. Ferrous Materials. Steel and Cast Iron. Springer Berlin, Heidelberg. 2008. 418 p. DOI: 10.1007/978-3-540-71848-2.
16. Totten G. E. Steel Heat Treatment Handbook. 2<sup>nd</sup> Edition. CRC Press, 2006. 1576 p.
17. ASM Handbook, Vol. 4: Heat Treatment. ASM International, American Society for Metals Park, Ohio. 1991. 2173 p.
18. ASM Handbook, Vol. 9: Metallography and Microstructures. ASM International, American Society for Metals Park, Ohio. 2004. pp. 493–512. DOI: 10.1361/asmhba0003752.
19. Kazakov A. A., Ryaboshuk S. V., Lyubochko D. A., Chigintsev L. S. Research on the Origin of Nonmetallic Inclusions in High-Strength Low-Alloy Steel Using Automated Feature Analysis. *Microscopy and Microanalysis*. 2015. Vol. 21, No. 3, pp. 1755–1756. DOI: 10.1017/S1431927615009551.
20. Kazakov A., Kovalev S., Ryaboshuk S. Metallurgical expertise as the base for determination of nature of defects in metal products. *CIS Iron and Steel Review*. 2007. Vol. 2, pp. 7–13.